

pubs.acs.org/Macromolecules

polarized light optical microscopy and differential scanning calorimetry (DSC). Simultaneous SAXS/WAXS real time results also revealed that PLLA-*b*-PCL copolymers are melt mixed for most compositions while blends of equivalent molecular weight homopolymers were found to be immiscible.^{20–23}

The thermally stimulated depolarization currents (TSDC) is a dielectric technique that has been previously applied to the study of blends miscibility when the components present dipolar molecular segments in their structure.^{24,25} Its resolution is very high due to its equivalent frequency which is in the range of millihertz.

In this work the structural, dielectric, and calorimetric behavior of the PDLLA/PCL blends is followed in the entire concentration range. A previous work on these same blends lead to the conclusion that the blends were immiscible but that the PCL addition had a plasticization effect as seen by a slight decrease in the storage modulus and a slight increase in the thermal stability.¹ The main objective of this work is to proceed to assess the previous results by using more sensitive techniques on this important blend system. The study of structural changes, crystallization, and variations on local and segmental molecular mobilities should lead to a better understanding of the interactions in the blends.

Experimental Section

Materials. The polymers used for the blends are poly-(ϵ -caprolactone) (PCL), supplied by Solvay, CAPA R FB100 with an approximate number-average molecular weight of 100 kg/mol, and a DL-lactide copolymer, labeled PDLLA, with 12 mol % of D-lactide isomer and a nominal molecular weight of 190 kg/mol; its trade name is Galastic, and it was kindly supplied by Galastic (Belgium). The choice of this copolymer, instead of neat PLLA, was made in order to avoid the crystallization of this component, which would increase the complexity of the results. The blends were prepared in an internal mixer from Rheomix-Haake PolyLab at 150 °C for 10 min, at velocities ranging from 20 to 100 rpm. The polymers were previously dried at 50 °C for 4 h. Compositions studied here are 100/0, 80/20, 64/36, 20/80, and 0/100.

After mixing, the material was removed from the chamber and allowed to cool down to room temperature. The blends were ground in a laboratory mill and dried again under vacuum (50 °C for 24 h). The dried powder was compression-molded in a Carver laboratory press at 120 °C into sheets with thicknesses varying from 160 to 350 μ m.

WAXS Experiments. The wide-angle X-ray scattering scans were performed in an X-Pert Panalytical automatic θ – 2θ diffractometer. The excitation voltage was 40 kV, and the tube current 40 mA for Cu K α radiation. The data acquisition was performed by steps of 0.02° and 2 s counting time from 10 to 35° in 2θ , at room temperature.

Differential Scanning Calorimetry (DSC). A Perkin-Elmer DSC-7 differential scanning calorimeter was employed. It was calibrated with indium and tin and ultrapure nitrogen was used as purge gas. Sample mass was kept approximately constant at 5 mg. Standard DSC cooling and heating runs were performed at 20 °C/min. The isothermal crystallization of the PCL component was also studied. In this case, the samples were heated to 100 °C and kept for 3 min at that temperature. Then they were quickly cooled (at a controlled rate of 60 °C/min) to the isothermal crystallization temperature T_c , at which the heat flow was recorded as a function of time (the samples were left to crystallize until saturation). The DSC isothermal crystallization procedure closely followed the recommendations given previously.²⁶

Thermally Stimulated Depolarization Currents Experiments (TSDC). The TSDC technique consists of polarizing a sample at a temperature where the dipolar species under study have a low relaxation time, quenching this polarization by lowering the

temperature to LN₂ temperature and recording the current due to the sample depolarization as the temperature is increased. The cryostat and the fully automated measuring system were designed in our laboratory. The disk-shaped sample, 20 mm in diameter and around 250 μ m thick, is located in the TSDC cryostat between two vertical metallic disks lightly spring-loaded. The polarization temperature, T_p , is chosen so as the dipoles under study would be mobile. An external electric field, $E_p = 1$ MV/m, is applied to the sample in a dry N₂ gas atmosphere (600 mTorr). Then, the sample is quenched to liquid nitrogen temperature, and the electric field is switched off. The cell is evacuated and filled with pure He gas which is the interchange gas, and the return to the random orientation state of the previously oriented dipoles is thermally stimulated by a temperature increase at a linear rate, $b = 0.07$ K s^{–1}, from 85 to 335 K. The depolarization current is digitally recorded by a Keithley 642 electrometer. The sensitivity of our system is 10^{–16} A. The current density peaks caused by the polarization decay due to each type of dipole occur at temperatures where the relaxation time of the dipolar species reaches the time scale of the experiment. The equivalent frequency for this dielectric experiment is estimated to be about 3 mHz. This low equivalent frequency results in a very good resolution for this technique. Another advantage of the TSDC technique is its capability to isolate a particular relaxation from its neighboring peaks by carefully choosing the polarization conditions.

All the TSDC curves presented here have been normalized to a polarizing field of 10⁶ V/m, an area of 10^{–4} m², and a thickness of 100 μ m.

Results and Discussion

X-ray Diffraction Results. The diffractograms obtained for the neat homopolymers and the three blend compositions are shown in Figure 1. PCL crystallizes at all compositions, and even though the neat PDLLA film is amorphous, as expected for a 12 mol % content of the D-enantiomer, crystallinity of PDLLA was unexpectedly detected in some of the blend samples. Both blend components crystallize in the orthorhombic $P2_12_12_1$ space group. The most intense Bragg peak for PDLLA is located at $2\theta = 16.69^\circ$, and it corresponds to the (110)/(200) reflections of the orthorhombic PLLA α -structure which cell parameters are $a = 10.66$ Å, $b = 6.16$ Å, and $c = 28.88$ Å.²⁷ This peak is clearly seen in the diffractograms recorded for the two richest PDLLA blends. PCL's parameters are $a = 7.496$ Å, $b = 4.974$ Å, and $c = 17.297$ Å.²⁸ For the 20/80 blend, weak traces of 3D order for PDLLA are still detected. The unexpected crystallinity of PDLLA, even though the average content of D-lactide was higher than 6%, is attributed to the plasticization effect of the PCL on PDLLA, a sign of molecular interaction, which increases the PDLLA chain mobility in PDLLA-rich regions. This result was corroborated by DSC, and a possible explanation for the reason why a PDLLA sample with 12% D-lactide can crystallize is also presented below. This plasticization effect on PDLLA (in terms of crystallinity development by the presence of an interacting highly mobile low- T_g component) has not been previously reported for this blend system.

The degree of crystallinity, X_c , was carefully determined by the deconvolution of the WAXS spectrum for each blend composition into the Bragg peaks of both structures plus the contributions of the broad amorphous halos of both components. A Pearson function was used to simulate the profiles both of the crystalline diffracted intensity (width much less than 1° in 2θ) and the amorphous halos (width covers several degrees in 2θ). The best fit to the experimental curve, made with the Profit software by Philips Analytical, provides a list of all the Pearson profiles with their height,

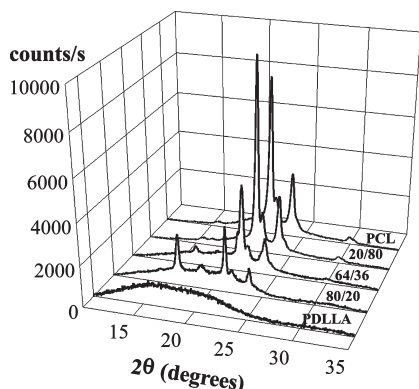


Figure 1. WAXS spectra for PDLLA/PCL blends with Cu K α radiation, $\lambda = 1.5418$ Å. The blend composition is indicated on each curve.

width, and area under the curves. The equivalent list from the diffraction of the neat homopolymers in amorphous and semicrystalline states is used to sort the contribution of each phase. The crystallinity degree of each component was calculated by the quotient of the area under the Bragg peaks over the area under both the crystalline and the amorphous contributions.

The variation of the crystallinity degree, in percent, as a function of the PCL corrected concentration in the blend (i.e., the composition of the amorphous zones of the blends) is presented in Figure 2. For the blend with the highest PCL content (80%) the crystallinity is higher than for the neat PCL films. The addition of small quantities of PDLLA may have a nucleating effect on PCL, thus increasing X_c from 42 to 56%. This could happen, even if the PDLLA component remains amorphous, by heterogeneity transfer to the PCL phase. As the rigid PDLLA chains become more abundant the PCL phase is now immersed in a matrix which imposes restrictions on the 3D ordering of the PCL chains. This reduced chain mobility decreases the PCL crystallinity to 24% for the 60/40 blend and further reduces it to 13% for the 80/20 blend. Simultaneously, the PDLLA crystallinity degree increases from 2 to 7% for blends with 60 and 80% of PDLLA nominal content, respectively.

Calorimetric Results. Figure 3a shows DSC first heating scans of all the samples prepared covering the temperature range available; no information on the glass transitions of the blend components was obtained. Two important features can be observed here. First, the endotherms located in the range between 300 and 345 K correspond to the melting of the PCL component in the blends. The peak melting temperature clearly decreases as the content of PDLLA in the blend increases; this feature is a sign of at least partial miscibility between the components. For immiscible blends, the melting point of the phases involved are expected to be invariant with composition.

The second peculiar result is that a small endotherm was detected for the blends in the temperature range between 375 and 400 K that clearly corresponds to the melting of the PDLLA phase. This is an unexpected result since it is widely reported in the literature that PDLLA samples with 12% D-lactide should be amorphous, since the random distributions of the D-lactide interrupt so frequently the crystallizable L-lactide sequences that no crystallization can develop.

In fact, Figure 3 shows that within the experimental uncertainty of the measurement the neat PDLLA sample is indeed 100% amorphous. As was described above, WAXS experiments corroborated that the neat PDLLA employed is indeed amorphous and that the blends contain a semicrystalline PDLLA phase. In a previous study that employed the

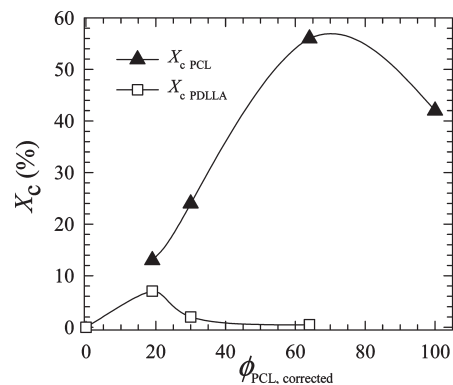


Figure 2. PDLLA and PCL crystallinity degrees as a function of the blend composition corrected by the crystallinity.

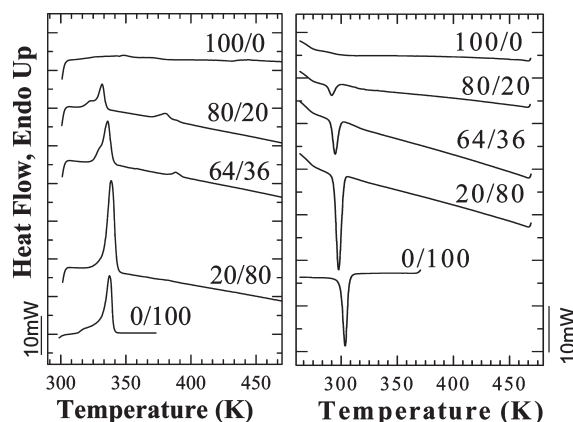


Figure 3. DSC scans (a) first heating and (b) first cooling for PDLLA/PCL. The global compositions are indicated above the traces.

same materials but mixed with nanoclays, it was assumed that the PDLLA was completely amorphous when pure or as a blend component, even though at the time no experiments were performed to specifically prove this point.¹

We interpret the development of crystallinity within the PDLLA phase as a result of its interaction with PCL that can cause increased chain mobility (since the PCL component has a low T_g value, see below) during sample storage at room temperature. Also, we speculate that the reported content of D-lactide by the manufacturer (12%) is probably an average value, and there would be a length distribution of the D-lactide sequences in the chains around this average value; it is then viable that those with a small content of this isomer within a specific distribution may be able to crystallize once they are plasticized by PCL, since they may have longer PLLA sequences. In any case the crystallinity developed by the PDLLA in the blends was quite small. In order to prove this assumption, a detailed study of the chain microstructure must be undertaken by for instance NMR, a study outside the scope of this paper.

Figure 3b shows the cooling DSC scans that immediately followed the first heating runs presented in Figure 3a. It is interesting to note that only the PCL phase can crystallize now, since no traces of PDLLA crystallization were found. The peak crystallization temperature was found to decrease as the PDLLA content in the blends increased, again a sign of partial miscibility. In order to try to crystallize the PDLLA-rich phase that could be forming in these blends, we performed slow cooling experiments in the DSC (at 5 and 1 °C/min), but no crystallization was detected. In fact, the second heating runs were very similar to those presented in Figure 3a, except for the absence of the melting peak in the

temperature range between 375 and 400 K (results not shown). We concluded that the crystallization of the PDLLA phase takes place slowly at room temperature during storage of the samples. No further experiments on the slow crystallizing PDLLA phase were performed, since the PCL phase crystallized much faster and in more significant amounts and therefore was easier to investigate.

The isothermal crystallization of the PCL-rich phase was studied by DSC. Figure 4 shows how the inverse of the half-crystallization time varies as a function of the isothermal crystallization temperature. This parameter is an experimentally determined value²⁶ that gives an idea of the overall crystallization rate of the PCL phase expressed in min^{-1} . In the case of immiscible blends where the content of the main crystallizing component (PCL in this case) exceeds 30%, no variation in the crystallization kinetics is expected, unless a special compatibilization technology is employed so that confined phases are generated that may have different nucleation mechanism than the homopolymers.²⁹

Figure 4, on the other hand, shows that the overall crystallization rate of the PCL phase is a function of the PDLLA content in the blends. In fact, a larger supercooling is needed for the crystallization of the blends than for the crystallization of neat PCL, and the difference is larger the higher the amount of PDLLA in the blends. This fact is consistent with the standard DSC behavior where upon dynamic cooling, the supercooling needed for crystallization was also higher as the PDLLA content in the blends increased (Figure 3b). Therefore, the isothermal crystallization also indicates that a certain degree of interaction between the components exists, so that the PCL chains are experiencing difficulty in nucleating and in diffusing to the crystallization front, since PDLLA chains which are less flexible are interacting with them. The coexistence of a PCL-rich phase and a PDLLA-rich phase would be consistent with these results.

In polarized light optical microscopy (PLOM) experiments, the PCL component within the blends developed negative spherulites as expected, with clear Maltese cross extinction patterns. The quantitative measurements of radial growth yielded spherulitic growth rate, G , results (not shown here) that also demonstrated that the G values of the PCL component in the blends were a function of the PDLLA content in a very similar way to the overall isothermal crystallization results. As the PDLLA content increased, the G decreased, indicating imposed restrictions on secondary nucleation that are consistent with the DSC findings and with PDLLA and PCL interactions.

TSDC Results. The low-temperature TSDC spectra given by the two homopolymers (lines) and the three blends (filled symbols) studied here are shown in Figure 5 in a temperature range from 85 to 180 K. The polarization temperature was always 150 K in order to isolate the local relaxations from the much more intense primary modes at higher temperatures. These spectra correspond to relaxations originated by local motions of the mobile dipolar entities in the amorphous phase, i.e., small oscillations of the carbonyl group. These local modes are not usually well resolved by dynamic-mechanical thermal analysis or broadband dielectric spectroscopy experiments. This temperature range does not include the onset of the cooperative phenomena which take place near the glass transition temperatures of the two blend components that will be discussed below.

It is readily seen that the intensity of the neat semicrystalline PCL band has a much higher intensity than that of the neat PDLLA, which is 100% amorphous. This indicates that, even for this low-amplitude motions, the flexibility of the main chains strongly affects the number of the mobile

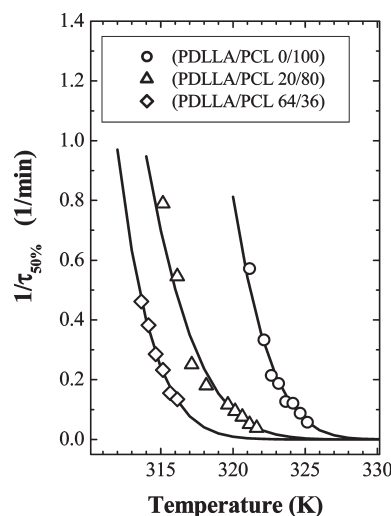


Figure 4. Crystallization rate expressed as the inverse of the experimentally determined half-crystallization time as a function of temperature. The solid lines are fittings to a modified version of the Lauritzen and Hoffman theory according to ref 28 and employing the following parameters (defined in ref 28): $a_0 = 4.5 \text{ \AA}$, $b_0 = 4.1 \text{ \AA}$, $\rho_c = 1.175 \text{ g/cm}^3$, $\rho_a = 1.090 \text{ g/cm}^3$, $\Delta H_m^0 = 139.5 \text{ J/g}$, $T_m^0 = 342.2 \text{ K}$, $T_g = 209 \text{ K}$, $T_\infty = 179 \text{ K}$.

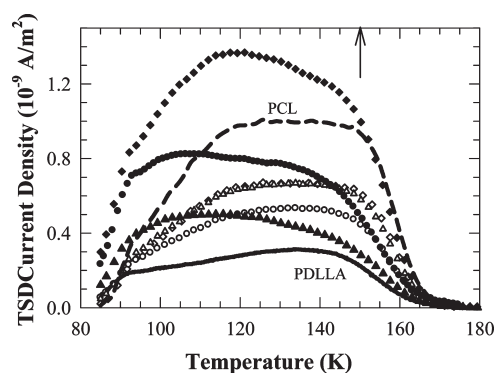


Figure 5. Low-temperature TSDC spectra for PDLLA/PCL: (—) 100/0, (●, ○) 80/20, (▲, △) 64/36, (◆, ◇) 20/80, (---) 0/100. Experimental: filled symbols; simulated: empty symbols. $T_P = 150 \text{ K}$.

entities that can orient in the amorphous phase in the presence of the electric field. The spectrum for the 20/80 blend composition is the most intense in Figure 5. It is to be noted that in the previous section we have shown that, for this composition, PCL has the highest crystallinity of all the samples studied here. If an additive law among the contribution of the two components were valid, the high intensity of this band could not be explained. This consideration is quantified in Figure 5 (open symbols) where we plot the curve calculated from the sum of the weighted contributions of the amorphous phase of each component according to the corrected blend composition. The profile and strength of the simulated curve corresponding to the 20/80 blend differ strongly from the experimental ones. The high number of orientable dipoles for this composition might be due to a huge effect of the 80% of PCL on the 20% of PDLLA which renders mobile the PDLLA dipoles whose motion was hindered in the rigid neat homopolymer, at least as far as the localized reorientations are concerned.

For the 64/36 and 80/20 compositions the intensities of the low-temperature signal are in better quantitative agreement with the increasing amount of PCL amorphous phase as PDLLA content increases. It is to be noted from Figure 5 that in these rich PDLLA blends the mode whose intensity is

most enhanced is the lowest temperature one, i.e., the relaxation of the shortest range reorientations.

The lack of additivity of the component contributions to the TSDC profiles of the blends for the localized relaxation modes can be taken as another proof of the existence of chain interactions between the blend components.

Because of the complexity of the material morphology, a broad distribution of relaxation times is expected in this multicomponent peak which is the sum of several modes (γ and β) from the two blend components. In order to have an estimate of these distribution parameters for the blends, the broad peak has been deconvoluted in Debye contributions by using the direct signal analysis³⁰ which was applied to the TSDC spectra of PLLA-*b*-PCL block copolymers.¹⁹ The relaxation time temperature variation of each Debye process in this multicomponent peak obeys an Arrhenius law $\tau(T) = \tau_0 \exp(E_A/kT)$, where E_A is the activation energy and τ_0 the inverse frequency factor. The activation energy histogram could be described by three Gaussian distributions (γ_1 , γ_2 , and β) whose mean values do not vary significantly with the blend composition for the two highest temperature distributions, i.e., γ_2 (0.34 ± 0.02 eV) and β (0.51 ± 0.02 eV). For the γ_1 mode there is an increase in the mean activation energy on going from neat PCL, 0.20 eV, to the richest PLLA blend, 0.25 eV. Additionally, the profile of the multicomponent low-temperature signal shows that the main change, when the profile of the blend peaks is compared to that of the homopolymers, is the enhancement of the γ_2 peak intensity, which is weak in both homopolymers. However, this growth of the lowest temperature mode is not as pronounced as in the block copolymers PLLA-*b*-PCL which are miscible in the amorphous phase (see Figure 3 in ref 19). Additionally, in the blends the β mode is less affected as compared to a large intensity decrease observed in the block copolymers which was explained in terms of the restrictions imposed on the homogeneous amorphous phase by the increase of the PLLA crystalline lamellae in the presence of PCL.

In the copolymers the amorphous zones are miscible as demonstrated by the variation with composition of the α transition temperatures of the two components which could be quantitatively accounted for by the self-concentration model for miscible blends when the two components have distant transition temperatures.³¹ The α TSDC modes are the dielectric manifestation of the onset of segmental mobilities, i.e., the glass transition of PCL and PLLA. Both peaks shift in the block copolymers as a function of composition, reducing the difference between their positions in temperature, thus evidencing the existence of two molecular dynamics, different from that of the homopolymers. However, the existence of two transition temperatures should not be interpreted any more as a signature of immiscibility.^{24,25} The self-concentration model for miscible blends quantitatively predicts this result in terms of chain connectivity.

The high-temperature TSDC spectra of the PDLLA/PCL blends, plotted in Figure 6, are made from the contributions of the α mode which are characteristic of cooperative mobilities, and around 270 K, of the Maxwell–Wagner–Sillars interfacial polarization peak present in the highly crystalline PCL.

When the blends are immiscible, the current peak temperature of the α modes should be that of the homopolymers; i.e., the T_g 's are unchanged. For neat PCL, the α peak is located at $T_{M\alpha PCL} = 207$ K, and it can be seen in Figure 6a that this peak exists for all compositions. It shifts to higher temperatures and broadens as the amount of PDLLA is increased. The maximum shift is +14 K for the 80/20 blend.

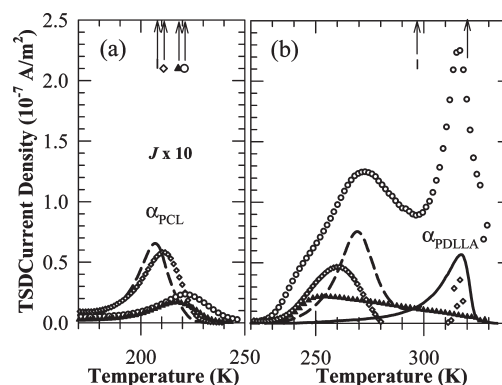


Figure 6. High-temperature TSDC spectra for PDLLA/PCL blends: (—) 100/0, (○) 80/20, (▲) 64/36, (◇) 20/80, (---) 0/100. (a) PCL α mode. (b) PDLLA α mode. The arrows indicate the polarization temperatures.

This shift proves the existence of a phase predominately composed of PCL chains, present at all compositions; this is in agreement with the partial miscibility and adhesion found previously for certain compositions by other techniques.⁹

From the area under the TSDC α mode the polarization can be calculated which is proportional to the number of oriented dipoles, i.e., the mobile amorphous phase. In Figure 7 (open symbols) the variation of the polarization of the PCL component is plotted as a function of the PCL amorphous phase concentration. The polarization should decrease as the amount of PCL amorphous phase diminishes. This is observed except for the 20/80 blend, which shows a comparable number of orientable dipoles as in the neat PCL. We might speculate that the PDLLA chains which are included in the PCL-rich phase contribute to the polarization as their motion is less hindered than in the rigid PDLLA phase.

The width of the α_{PCL} mode at half height monotonously increases from 16.9 K for pure PCL to 26.6 K for the 80/20 blend. The change in the profile of the α mode of PCL evidence a wider distribution of relaxation times as the PDLLA amount increases. This last result together with the variation of the T_{gPCL} might be taken as proof of the existence of a certain degree of miscibility among the blend components.

The SADSA procedure³² was applied to PCL α mode in order to calculate the relaxation parameters which characterize the VTF relaxation time, $\tau_{VTF}(T)$, which is the best approach for segmental relaxations:

$$\tau_{VTF}(T) = \tau_{0VTF} \exp \left[\frac{E_{VTF}}{k(T - T_{VTF})} \right]$$

This analysis is based on the decomposition of the global peak into elementary Debye contributions, and a simulated annealing procedure together with a Monte Carlo algorithm is used for finding the best fit to the experimental curve. The best fit for all the blends was reached for a VTF energy within 0.140 ± 0.005 eV, and a common $T_{VTF} = 150 \pm 2$ K. An example of the fitting is given in Figure 8 for the 80/20 blend.

The relevant variation among the relaxation parameters of the PCL α mode was found in the regular increase in the pre-exponential factor, τ_{0VTF} , which varied from 3×10^{-11} to 10^{-8} s on going from the 0/100 to the 80/20 blend.

The PDLLA α mode is observed in Figure 6b at 317 K for the homopolymer and at 315 K for the 80/20 blend. The -2 K shift observed for the T_{gPDLLA} for this blend is an indication of some weak interactions of the PDLLA amorphous chains with the PCL chains, even though previous

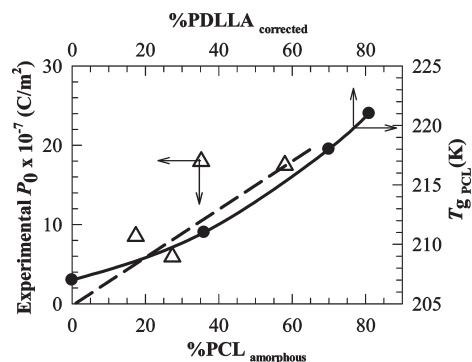


Figure 7. T_g variation of PCL in the PDLLA/PCL blends as a function of the PDLLA content (●), top and right axis. Variation of the α_{PCL} mode polarization as a function of the amorphous PCL concentration (Δ), bottom and left axis.

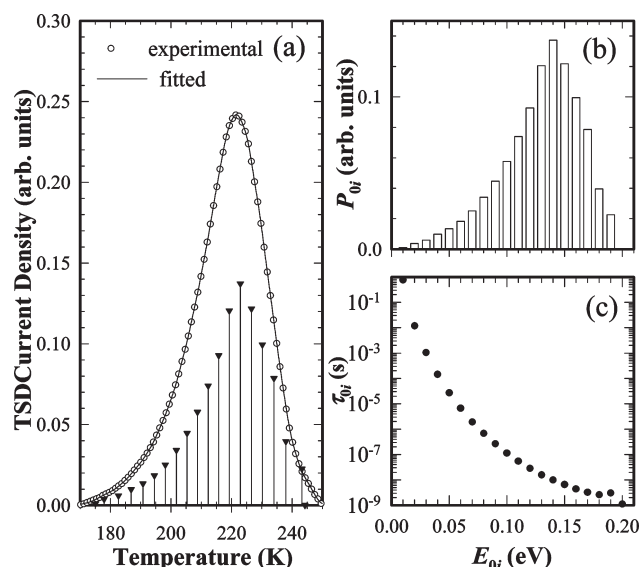


Figure 8. Simulated annealing direct signal analysis of the α mode of the 80/20 PLLA/PCL blend: (a) TSDC trace and positions on the temperature axis of the Debye modes. (b) Energy histogram of the contributions to the total polarization. (c) Variation of the VTF pre-exponential factor as a function of the activation energy of each Debye mode.

works have reported invariability of the T_{gPDLLA} when PCL is added.^{14,15} In the miscible block copolymers PLLA-*b*-PCL at this same concentration the TSDC α_{PLLA} mode had already shifted -35 K. A more quantitative indication of the decreased miscibility in the blend as compared to the block copolymer is the self-concentration parameter of PCL in the blend which could be estimated $\phi_{SPCL} = 79\%$, which is intermediate between the values found for PCL in the copolymer. For the PDLLA component in the block copolymer a value of 31% was calculated where as with the two points available in the blends the self-concentration is very near 100%.

The intensity of the α mode, which in neat PDLLA was weak, increases as 20% of the more flexible PCL is added, even though the PDLLA amorphous phase is depleted by the appearance of crystalline order at this composition. These two results might be attributed to the effect of the addition of PCL chains to the amorphous PDLLA phase, which renders an existing rigid amorphous phase mobile, allowing the chain folding and the cooperative motions possible in this phase.

It is worth noting the presence of an intense complex mode in the 250–270 K region, whose strength is maximum when

the PDLLA crystallinity reaches the highest value, i.e., the 80/20 blend. This mode is similar to the interfacial polarization relaxation which is present in semicrystalline PCL attributed to the charge accumulation of carriers at the crystal–amorphous interphase. As the crystallinity degree decreases, the peak becomes wider and weaker, indicating a broad distribution of relaxation times, i.e., a variety of dipolar species.

In the 64/36 blend the α_{PDLLA} mode covers a wide temperature range, from 230 to 330 K, thus evidencing the existence of a broad distribution of compositions. These concentration fluctuations have been reported previously in PCL blended with polycarbonate³³ and attributed to a partial miscibility among the blend components. It is to be noted that this exact composition has been reported by Meredith and Amis,³⁴ as the critical point at a temperature of 359 K of the LCST phase boundary obtained by cloud point determinations. This concentration is then the most favorable for observing the dynamics that differ the most from those of the neat homopolymers. The shift of the two α peaks in this blend is the most relevant as seen in Figure 6b. As compared to the PLLA-*b*-PCL copolymers, the α modes temperature shifts in the blends are much weaker, showing a partial miscibility, whereas in the former, the considerable shifts could be quantitatively explained¹⁹ by the self-concentrations model for miscible blends.³⁰

For the 20/80 blend we were not able to record anything beyond the interfacial peak as the fusion of the abundant PCL crystalline phase coincides with the PDLLA glass transition and the signal becomes unstable due to the sample transformation.^{14–16}

In order to study the morphology of the blends, fracture surfaces performed in liquid nitrogen have been investigated by scanning electron microscopy (SEM). These micrographs differ from the typical island–sea images given by immiscible blends where the two-component phases are clearly observed, for example in the SEM microphotographs of PLA/PCL blends by Wu et al.³⁵ In our case, at the scale of the picture, we were not able to detect the presence of two phases.

Conclusion

The accumulated results on PDLLA/PCL blends of a variety of experiments, such as WAXS, DSC, TSDC, PLOM, and SEM, show that these melt-mixed blends present a certain degree of miscibility as the coexistence of a PCL-rich phase and a PDLLA phase has been demonstrated. The evidence gathered here does not sustain the existence of two completely segregated phases (as usually seen in immiscible polymer blends). The first evidence is the PCL plasticization effect of this component on PDLLA which allows the crystallization of the latter even though the ratio of D- to L-enantiomer seemed to be high enough to forbid the 3 D order. The decrease of the PCL melting and crystallization temperatures as the PDLLA concentration increases also reveals the existence of chain interactions. The PCL isothermal crystallization is also retarded in the blends as compared to the homopolymer at a given temperature. SEM micrographs do not show a distinct two phases morphology with particles dispersed in a matrix. The dielectric relaxations show some common features with the TSDC results obtained on block copolymers PLLA-*b*-PCL. First, the short-range local motions at the origin of the secondary relaxations do not agree neither in profile nor in strength with an additive contribution of the neat components signal according to the composition of the amorphous regions of the blends. The changes observed follow the same trend as in the block copolymers but with less pronounced effects. As to the

primary relaxation modes, associated with the glass transition temperature, a small shift is recorded for the α peak of the PCL toward high temperature, demonstrating a slight rigidization of the PCL amorphous regions attributed to the presence of PDLLA chains. Additionally, the PCL crystallinity of the 20/80 blend is higher than that of neat PCL, owing to an increased number of crystallization nuclei. The PDLLA-rich regions which are semicrystalline have segmental dynamics which for the lower PCL content are slightly accelerated while at intermediate PCL concentrations the relaxation time distribution is very wide, thus indicating strong concentration fluctuations, which confirm the partial miscibility of these blends.

Acknowledgment. Financial support from FONACIT (Proyectos G2005-000776 and F-2005-000284) is highly acknowledged.

References and Notes

- (1) Cabedo, L.; Feijoo, J. L.; Villanueva, M. P.; Lagarón, J. M.; Gimenez, E. *Macromol. Symp.* **2006**, *233*, 191.
- (2) Kister, G.; Cassanas, G.; Bengounhon, M.; Hoarau, D.; Vert, M. *Polymer* **2000**, *41*, 925.
- (3) Moe, K. S.; Weisman, R. A. *Laryngoscope* **2001**, *111*, 1697.
- (4) Langer, R.; Vacanti, J. P. *Tissue Eng. Sci.* **1993**, *260*, 920.
- (5) Wittwer, G.; Adeyemo, W. H.; Voracek, M.; Turhani, D.; Ewer, R.; Watzinger, F.; Enislidis, F. *Oral Maxillofac. Surg.* **2005**, *100*, 656.
- (6) Powell, H. M.; Ayodeji, O.; Summerfield, T. L.; Powell, D. M.; Kniss, D. A.; Tomasko, D. L.; Lannutti, J. L. *Biomaterials* **2007**, *28*, 5562.
- (7) Steendam, R.; van Steenberger, M. J.; Hennink, W. E.; Frijlink, H. W.; Lerk, C. F. J. *J. Controlled Release* **2001**, *70*, 71.
- (8) Nieminen, T.; Kallela, I.; Keranen, J.; Hiidenheimo, I.; Kainulainen, H.; Wuolijoki, E.; Rantala, I. *Int. J. Oral Maxillofac. Surg.* **2006**, *35*, 727.
- (9) Aslan, S.; Calandrelli, L.; Laurienzo, P.; Malinconico, M.; Migliaresi, C. *J. Mater. Sci.* **2000**, *35*, 1615.
- (10) Schindler, A.; Jeffcoat, R.; Kimmel, G. L.; Pitt, C. G.; Wall, M. E.; Zweidinger, R. A. In *Contemporary Topics in Polymer Science*; Pearce, E. M., Schaefgen, J. R., Eds.; Plenum Pub. Corp.: New York, 1977; Vol 2, p 251.
- (11) Potts, J. E.; Clendinning, R. A.; Cohen, S. *Tech. Pap.—Soc. Plast. Eng.* **1975**, *21*, 567.
- (12) Chen, C.-C.; Chueh, J.-Y.; Tseng, H.; Huang, H.-M.; Lee, S.-Y. *Biomaterials* **2003**, *24*, 1167.
- (13) Sivalingam, G.; Vijayalakshmi, S. P.; Madras, G. *Ind. Eng. Chem. Res.* **2004**, *43*, 7702.
- (14) Na, Y.; He, Y.; Shuai, X.; Kikkawa, Y.; Doi, Y.; Inoue, Y. *Biomacromolecules* **2002**, *3*, 1179.
- (15) Broz, M. E.; VanderHart, D. L.; Washburn, N. R. *Biomaterials* **2003**, *24*, 4181.
- (16) Tsuji, H.; Ikada, Y. *J. Appl. Polym. Sci.* **1996**, *60*, 2367.
- (17) Leiva, A.; Gargallo, L.; González, A.; Araneda, E.; Radic, D. *Eur. Polym. J.* **2006**, *42*, 316.
- (18) Calandrelli, L.; Calarco, A.; Laurienzo, P.; Malinconico, M.; Petillo, O.; Peluso, G. *Biomacromolecules* **2008**, *9*, 1527.
- (19) Laredo, E.; Prutsky, N.; Bello, A.; Grima, M.; Castillo, R. V.; Muller, A. J.; Dubois, Ph. *Eur. Phys. J. E* **2007**, *23*, 295.
- (20) Hamley, W.; Castelletto, V.; Castillo, R. V.; Muller, A. J.; Martin, C. M.; Pollet, E.; Dubois, Ph. *Macromolecules* **2005**, *38*, 463.
- (21) Hamley, I. W.; Parras, P.; Castelletto, V.; Castillo, R. V.; Muller, A. J.; Pollet, E.; Dubois, Ph.; Martin, C. M. *Macromol. Chem. Phys.* **2006**, *207*, 941.
- (22) Muller, A. J.; Balsamo, V.; Arnal, M. L. *Lect. Notes Phys.* **2007**, *714*, 229.
- (23) Castillo, R. V.; Muller, A. J. *Prog. Polym. Sci.* **2009**, in press.
- (24) Herrera, D.; Zamora, J. C.; Bello, A.; Grima, M.; Laredo, E.; Muller, A. J.; Lodge, T. *Macromolecules* **2005**, *38*, 5109.
- (25) Balsamo, V.; Newman, D.; Gouveia, L.; Herrera, L.; Grima, M.; Laredo, E. *Polymer* **2006**, *47*, 5810.
- (26) Lorenzo, A. T.; Arnal, M. L.; Albuern, J.; Muller, A. J. *Polym. Test.* **2007**, *26*, 222.
- (27) Sasaki, S.; Asakura, T. *Macromolecules* **2003**, *36*, 8385.
- (28) Bittiger, H.; Marchessault, R. H.; Niegisch, W. D. *Acta Crystallogr. B* **1970**, *26*, 1923.
- (29) Muller, A. J.; Balsamo, V.; Arnal, M. L. *Adv. Polym. Sci.* **2005**, *190*, 1.
- (30) Aldana, M.; Laredo, E.; Bello, A.; Suarez, N. *J. Polym. Sci., Part B: Polym. Phys.* **1994**, *32*, 2197.
- (31) Lodge, T. P.; McLeish, T. C. B. *Macromolecules* **2000**, *33*, 5278.
- (32) Laredo, E.; Bello, A.; Hernández, M. C.; Grima, M. *J. Appl. Phys.* **2001**, *90*, 5721.
- (33) Hernández, M. C.; Laredo, E.; Bello, A.; Carrizales, P.; Marcano, L.; Balsamo, V.; Grima, M.; Muller, A. J. *Macromolecules* **2002**, *35*, 7301.
- (34) Meredith, J. C.; Amis, E. J. *Macromol. Chem. Phys.* **2000**, *201*, 733.
- (35) Wu, D.; Zhang, Y.; Zhang, M.; Yu, W. *Biomacromolecules* **2009**, *10*, 417.